ISSN 1674-1056
http://cpb.iphy.ac.cn
http://iopscience.iop.org/cpb
中国物理 B
Chinese Physics
中国物理 Chinese Physics B

# Optical-induced dielectric tunability properties of DAST crystal in THz range

De-Gang Xu(徐德刚)[1,2], Xian-Li Zhu(朱先立)[1,2], Yu-Ye Wang(王与烨)[1,2], Ji-Ning Li(李吉宁)[1,2], Yi-Xin He(贺奕歆)[1,2], Zi-Bo Pang(庞子博)[3], Hong-Juan Cheng(程红娟)[3], Jian-Quan Yao(姚建铨)[1,2]

**Citation:**Chin. Phys. B . 2019, 28(12): 127701 . **doi:** 10.1088/1674-1056/ab4e81
Journal homepage: http://cpb.iphy.ac.cn; http://iopscience.iop.org/cpb

**What follows is a list of articles you may be interested in**

---

## Single-layer broadband planar antenna using ultrathin high-efficiency focusing metasurfaces

Hai-Sheng Hou(侯海生), Guang-Ming Wang(王光明), Hai-Peng Li(李海鹏), Wen-Long Guo(郭文龙), Tang-jing Li(李唐景), Tong Cai(蔡通)

Chin. Phys. B . 2017, 26(5): 057701 . **doi:** 10.1088/1674-1056/26/5/057701

## Study on the dielectric properties of Mg-doped $NaBiTi_6O_{14}$ ceramics

Yong Chen(陈勇), Simin Xue(薛思敏), Qian Luo(骆迁), Huyin Su(苏虎音), Qi Chen(陈琪), Zhen Huang(黄镇), Linfang Xu(徐玲芳), Wanqiang Cao(曹万强), Zhaoxiang Huang(黄兆祥)

Chin. Phys. B . 2017, 26(4): 047701 . **doi:** 10.1088/1674-1056/26/4/047701

## Dielectric and piezoelectric properties of (110) oriented $Pb(Zr_{1-x}Ti_x)O_3$ thin films

Jian-Hua Qiu(邱建华), Zhi-Hui Chen(陈智慧), Xiu-Qin Wang(王秀琴), Ning-Yi Yuan(袁宁一), Jian-Ning Ding(丁建宁)

Chin. Phys. B . 2016, 25(5): 057701 . **doi:** 10.1088/1674-1056/25/5/057701

## Piezoelectric and electro—optic properties of tetragonal $(1-x)Pb(Mg_{1/3}Nb_{2/3})O_3—xPbTiO_3$ single crystals by phenomenological theory

Qiu Jian-Hua, Wang Xiu-Qin, Yuan Ning-Yi, Ding Jian-Ning

Chin. Phys. B . 2015, 24(7): 077701 . **doi:** 10.1088/1674-1056/24/7/077701

## Dielectric and ferroelectric properties of $Sr_4CaSmTi_3Nb_7O_{30}$ with tetragonal tungsten bronze structure

Gong Gao-Shang, Fang Yu-Jiao, Huang Shuai, Yin Chong-Yang, Yuan Song-Liu, Wang Li-Guang

Chin. Phys. B . 2014, 23(9): 097701 . **doi:** 10.1088/1674-1056/23/9/097701

---

# Optical-induced dielectric tunability properties of DAST crystal in THz range*

De-Gang Xu(徐德刚)[1,2], Xian-Li Zhu(朱先立)[1,2], Yu-Ye Wang(王与烨)[1,2,†], Ji-Ning Li(李吉宁)[1,2], Yi-Xin He(贺奕欣)[1,2], Zi-Bo Pang(庞子博)[3], Hong-Juan Cheng(程红娟)[3], and Jian-Quan Yao(姚建铨)[1,2]

[1] *Institute of Laser and Optoelectronics, School of Precision Instrument and Opto-electronics Engineering, Tianjin University, Tianjin* 300072, *China*
[2] *Key Laboratory of Opto-electronic Information Technology (Tianjin University), Ministry of Education, Tianjin* 300072, *China*
[3] *The 46th Research Institute of China Electronic Technology Group Corporation, Tianjin* 300220, *China*

(Received 23 August 2019; revised manuscript received 27 September 2019; published online 29 November 2019)

The optical-induced dielectric tunability properties of DAST crystal in THz range were experimentally demonstrated. The DAST crystal was grown by the spontaneous nucleation method (SNM) and characterized by infrared spectrum. With the optimum wavelength of the exciting optical field, the transmission spectra of the DAST crystal excited by 532 nm laser under different power were measured by terahertz time-domain spectroscopy (THz-TDS) at room temperature. The transmitted THz intensity reduction of 26 % was obtained at 0.68 THz when the optical field was up to 80 mW. Meanwhile, the variation of refractive index showed an approximate quadratic behavior with the exciting optical field, which was related to the internal space charge field of photorefractive phenomenon in the DAST crystal caused by the photogenerated carrier. A significant enhancement of 13.7 % for THz absorption coefficient occurred at 0.68 THz due to the photogenerated carrier absorption effect in the DAST crystal.

**Keywords:** THz wave, organic DAST crystal, photogenerated carrier, dielectric property

**PACS:** 77.22.–d, 66.30.hd, 61.05.cp **DOI:** 10.1088/1674-1056/ab4e81

## 1. Introduction

Organic nonlinear optical (NLO) materials have attracted significant attention due to their potential for various applications, such as electro-optic modulation,[1] nonlinear frequency conversion,[2,3] optical data storage,[4,5] and optical telecommunication.[6] Especially in the field of THz technology, the organic NLO materials with excellent nonlinear optical and electro-optical (EO) properties have been considered to be the ideal media for efficient generation and sensitive detection of THz wave. Among the general materials, organic ionic salt 4-N, N-dimethylamino-4′-N′-methylstilbazolium tosylate (DAST) has drawn great interest due to its excellent properties, including large second-order nonlinear coefficient ($d_{11} = 1010\pm110$ pm/V, $\lambda = 1318$ nm),[7] low dielectric constant ($\varepsilon = 5.2$),[8] large electro-optical coefficient ($r_{11} = 92\pm9$ pm/V at $\lambda = 720$ nm),[9] and high laser damage threshold (2.5 GW/cm$^2$ at $\lambda = 1550$ nm).[10] It has been widely used in THz generation by optical rectification (OR)[11] and difference frequency generation (DFG)[12] as well as the THz detection by frequency up-conversion.[13]

Organic DAST crystal shows a non-centrosymmetric macroscopic crystal packing, which consists of a stilbazolium cation with positive charge and a tosylate anion with negative charge, connected by the strong Coulomb force.[14,15] It belongs to the monoclinic crystal (space group $Cc$, point group $m$, $z = 4$) with the lattice parameters of $a = 10.365$ Å, $b = 11.322$ Å, $c = 17.893$ Å, and $\beta = 92.2°$.[16] The D–$\pi$–A is a typical chromophore structure in DAST crystal, which is composed of a dimethylamino group (D), a pyridine group (A), and a $\pi$-conjugated bridge of C=C bond.[17,18] When a DAST crystal with the bandgap of 2.33–3.3 eV is excited by an optical field, the efficient charge transfer between donor and acceptor through the $\pi$-conjugated bridge could be beneficial to the generation of photogenerated carrier.[19] Thus, the dielectric properties of the DAST crystal may be changed. However, to date there has been no detailed study on the dielectric properties of DAST crystal in THz range under optical irradiation.

In this paper, the optical-induced dielectric tunability properties of DAST crystal in THz range were experimentally investigated. The DAST crystal was grown by the spontaneous nucleation method (SNM) and characterized by infrared spectrum. The optimum wavelength of the exciting optical field was chosen based on the stimulation of photocurrent. The transmission spectra of the DAST crystal under different power of 532 nm laser irradiation were measured at room temperature by terahertz time-domain spectroscopy (THz-TDS). The transmitted THz intensity reduction of 26% at 0.68 THz was obtained when the optical field was up to 80 mW, which could originate from the optically induced free carrier absorption effect in the DAST crystal. Moreover, the photorefractive

*Project supported by the National Basic Research Program of China (Grant No. 2015CB755403) and the National Natural Science Foundation of China (Grant Nos. 61775160, 61771332, 61705162, 51472251, and U1837202).

†Corresponding author. E-mail: yuyewang@tju.edu.cn

© 2019 Chinese Physical Society and IOP Publishing Ltd 

phenomenon and the absorption enhancement were observed in the DAST crystal under the irradiation of 532 nm laser field. It is expected that the DAST crystal with dielectric tunability properties can be further used to control the Fano resonances and applied in the fields of THz modulation, biosensing, and detection.[20,21]

## 2. Methods

### 2.1. Sample preparation and characterization

The growth material of the DAST crystal was synthesized from the organic compounds of 4-picoline, methyl toluenesulfonate and 4-N, N-dimethylamino-benzal-dehyde. The piperidine was chosen as the catalyst to promote the chemical synthesis, and methanol (99.9%) was used as the reaction solvent. Because the purity of the DAST material was directly determined by the quality of crystal growth, the crystalline powders of DAST were purified by a filter and recrystallization two times from methanol. The spontaneous nucleation method was adopted to prepare the DAST crystal by slow cooling in the range of 43–37 °C. The DAST growth solution was prepared in 600 ml methanol with 21 g purified DAST crystalline powder and was kept in the heating equipment for 3 h at 55 °C to ensure complete dissolution. The prepared DAST growth solution was transferred to a crystallizing bottle which was placed in a water bath, as shown in Fig. 1(a). The temperature adjustment accuracy in the water bath was kept at 0.01–0.03 °C. After keeping the water bath temperature at 50 °C for 24 h to stabilize the growth solution, the DAST crystal was grown under the cooling rate of 0.35 °C/day. Figure 1(b) shows a DAST crystal with a size of 5 mm×6 mm×0.35 mm after 12 days. The structure of the DAST crystal was characterized by an x-ray single crystal diffractometer (D/MAX-2500) with a scanning range of 5°–40° and a scanning speed of 1 °/min. The infrared spectrum of the DAST crystal was measured by an infrared spectrometer (Nicotron 6700) in the wavelength range of 400–4000 $cm^{-1}$.

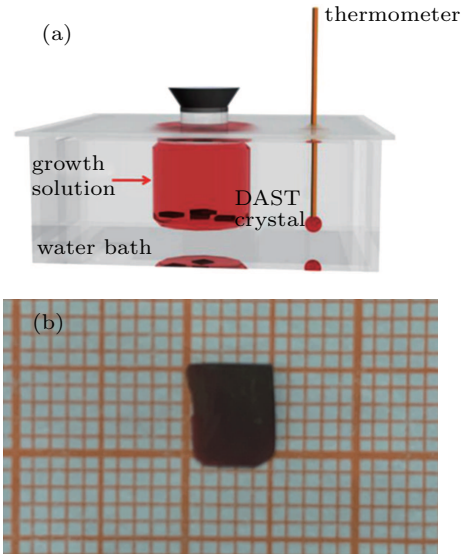



**Fig. 1.** (a) Growth device of spontaneous nucleation method. (b) Photograph of a DAST crystal with a size of 5 mm×6 mm×0.35 mm.

### 2.2. Experimental setup

Figure 2 shows the experimental setup. The dielectric properties of the DAST crystal under different power of 532 nm laser irradiation were demonstrated using THz-TDS with signal-to-noise ratio of 60 dB. The THz-TDS was driven by two erbium-doped fiber lasers (50 MHz, 50 fs, 1.55 μm). One of the fs fiber lasers was used to pump the photo-conductive antenna (PCA) emitter for the generation of the THz wave, and the other was used for the coherent detection of the THz wave. The time delay was dominated by electrical phase control. The measured frequency spectral resolution of the THz-TDS system was 3.8 GHz, and the diameter of the THz spot was 4 mm. In our experiment, the DAST crystal was vertically placed on the sample stage, and the transmitted time-domain THz pulses were collected. A 532 nm CW laser with the maximum power of 100 mW was employed to provide the exciting optical field. The 532 nm laser was expanded by a pair of lenses ($f = 150$ mm) and obliquely irradiated on the (001) surface of the DAST crystal at an angle of 45°, overlapping the spot of the THz wave. Every measurement under different irradiation power was repeatedly tested 3 times with the setting of 1024 times scan for each measurement. All spectra were conducted by averaging the values from several measurements. All the experiments were performed at room temperature with dry air purge (almost 0% relative humidity).

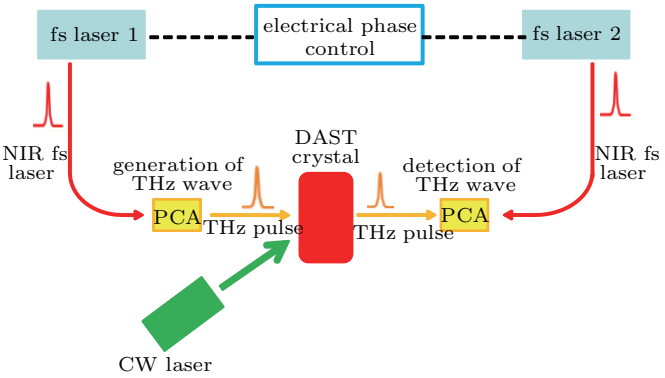



**Fig. 2.** Schematic diagram of the experimental setup.

## 3. Results and discussion

Figure 3 shows the x-ray diffraction spectrum of the self-growth DAST crystal. It was clearly demonstrated that the main diffraction peaks were between 9° and 30°. The three characteristics peaks centered at 9.90°, 19.86°, and 30.00° were assigned to the (002), (004), and (006) planes of the DAST crystal, with the full widths at half-maximum (FWHM)

of 12 arcsec, 24 arcsec, and 16 arcsec, respectively, which was consistent with the results reported by Teng.[22]

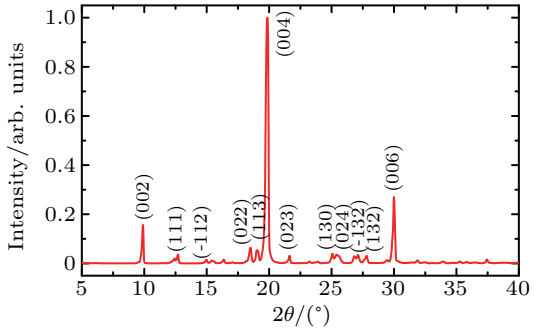



**Fig. 3.** X-ray diffraction spectrum of the self-growth DAST crystal.

The infrared spectrum of the self-growth DAST crystal is displayed in Fig. 4. The numerous characteristic infrared absorption peaks of the DAST crystal were assigned as follows:[23,24] the deformation vibration absorption of benzene ring C–H was at 3032 $cm^{-1}$; the olefin C=C stretching vibration absorption was at 1646 $cm^{-1}$; the stretching vibration absorption of pyridine ring C–N and benzene ring C–N were at 1531 $cm^{-1}$ and 1346 $cm^{-1}$, respectively; the anti-symmetric stretching vibration absorption of $SO_3$ was at 1161 $cm^{-1}$; the vibration absorption of C–H out-palne in benzene ring was at 999 $cm^{-1}$; the vibration absorptions of aromatic ring with 1, 4 substitutions were at 816 $cm^{-1}$ and 891 $cm^{-1}$, respectively; the bending vibration absorption of benzene ring was at 675 $cm^{-1}$; and the twisting vibration absorption of methyl groups C–H was at 567 $cm^{-1}$. The aldehyde band of 2720 $cm^{-1}$ was not observed in the infrared spectrum, which showed that there was no nonreacted materials in the DAST crystal. The locations of the main absorption peaks in the infrared spectrum were corresponding to the vibration modes of the DAST chromophore groups, which indicated that the impurities were few in the DAST crystal.

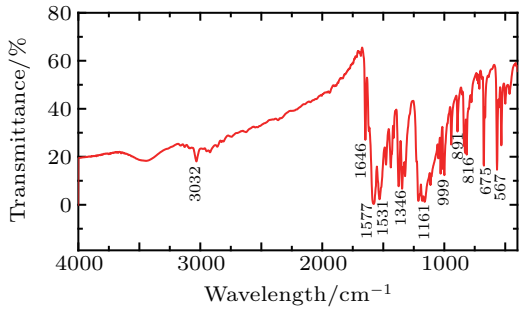



**Fig. 4.** Infrared spectrum of the self-growth DAST crystal.

To determine the optimum wavelength of the exciting optical field, the absorption spectrum of the DAST crystal in the wavelength range of 300–2000 nm was measured by a grating spectrometer (Omni-λ-3007), as shown in Fig. 5. The absorption of the DAST crystal reached nearly 90% in the band from 400 nm to 600 nm, which meant that the effective exciting wavelength of carrier was located in this range. Meanwhile, in order to estimate the density of excited carrier in the DAST crystal, the optoelectronic properties of the DAST crystal were measured under different wavelengths, which were emitted from 532 nm, 808 nm, and 1177 nm CW lasers, as shown in the inset of Fig. 5. When there was no irradiation, the dark current was relatively small and increased with the applied voltage. When the DAST crystal was irradiated by the CW laser, the trend of conduction current excited by 808 nm and 1177 nm laser had a slight change compared to that of dark current, and the maximum optoelectronic response was observed under 532 nm laser. Under the same pump power of 20 mW, the photocurrent in the DAST crystal excited by 532 nm laser was nearly 2 times of that excited by 808 nm and 1177 nm laser, which indicated that more photogenerated carrier was excited in the DAST crystal by 532 nm laser. It was consistent with the results of absorption spectrum of the DAST crystal. Therefore, the wavelength of the exciting optical field for the DAST crystal was chosen to be 532 nm due to the higher excitation efficiency of free carrier.

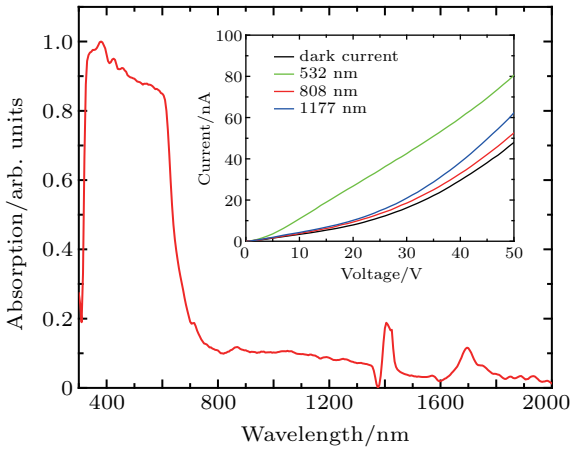



**Fig. 5.** The absorption spectrum of DAST crystal in the wavelength range of 300–2000 nm. Inset shows the photocurrent in DAST crystal excited by 532 nm, 808 nm, and 1177 nm CW lasers.

With the 532 nm laser excitation, the THz transmission spectra of the DAST crystal were investigated by THz-TDS. Figure 6(a) shows the THz time domain signal under different pump power. The detailed results in the black square are shown in the inset. It can be seen that the intensity of the transmitted THz wave decreased monotonically when the pump power increased from 0 mW to 80 mW. The phase of the transmitted THz wave shifted forward about 0.04 ps, which was related to the dielectric parameters change of the DAST crystal caused by the optical excitation. Based on the Fourier transform of the THz temporal signal, the THz frequency domain spectrum was obtained, as depicted in Fig. 6(b). At 0.5 THz, the intensity of the transmitted THz wave was lower due to the lattice vibration absorption of the DAST crystal. With

the increase of the frequency, the intensity of the transmitted THz wave showed a trend of increasing first and then decreasing, which was mainly originated from the strong absorption caused by the transverse optical phonon vibration of the DAST crystal anion-cation pairs at 1.0 THz.[25] In addition, when the power of 532 nm laser increased, the intensity of the transmitted THz wave dropped down. The maximum variation of the transmitted THz intensity induced by the optical field was found at 0.68 THz. It can be inferred that the DAST crystal can modulate the amplitude of THz wave by the optical induced method. As the DAST crystal has the same D–$\pi$–A structure with solar organic thin film materials, the exciton theory can be used to explain the mechanism of the change of the transmitted THz intensity in the DAST crystal under optical excitation.[26,27] When the photons of 532 nm laser were absorbed by impurities and detects in the DAST crystal, the strongly bound electron–holes pairs (neutral singlet excitons) instantly formed in the donor. The singlet excitons could diffuse to the interface of donor–acceptor and then formed charge transfer excitons because of the segregation of donor and acceptor in the DAST crystal. When the Coulomb binding energy was overcome by the molecular vibrational energy, the charge transfer excitons could be dissociated and then formed a conduction current, as measured in the inset of Fig. 5, which was also known as photogenerated carrier. The THz absorption by the photogenerated carrier in the DAST crystal resulted in the decrease of the transmitted THz intensity.

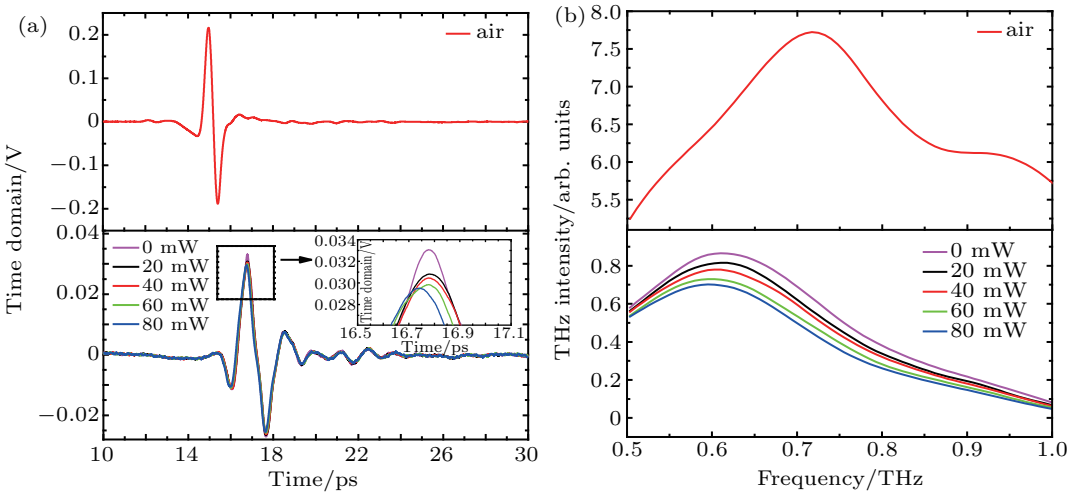



**Fig. 6.** (a) THz time-domain transmission spectrum through DAST crystal excited by 532 nm laser at different power. (b) Frequency-domain spectrum based on Fourier transform.

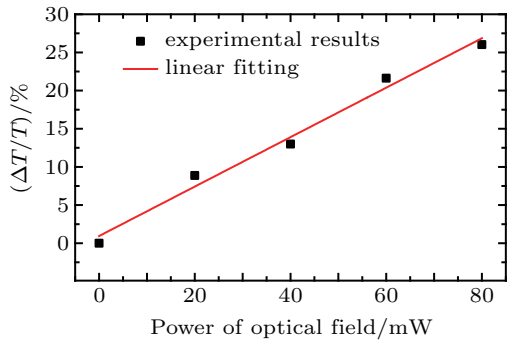



**Fig. 7.** The relationship between the variation rate of transmitted THz intensity and the power of optical field at 0.68 THz.

To evaluate the variation of the transmitted THz intensity with optical excitation, the variation rate of the transmitted THz intensity is defined by the formula $\Delta T/T = |T(I) - T(0)|/T(0) \times 100\%$, where $T(I)$ and $T(0)$ are the transmitted THz intensity with and without 532 nm laser field, respectively. Figure 7 shows the relationship between the variation rate of the transmitted THz intensity and the power of the optical field at 0.68 THz. It can be seen that the variation rate of the transmitted THz intensity increased linearly with the optical field power. The transmitted THz intensity reduction of 26% at 0.68 THz was obtained when the 532 nm laser power was up to 80 mW. Moreover, there was little transmitted 532 nm laser behind the DAST crystal during the process. It was deduced that the penetration depth of 532 nm laser in the DAST crystal was less than or close to the thickness of the sample 0.35 mm. Considering there was no saturation effect observed in our experiment, it was reasonable to infer that the transmitted THz intensity could be further reduced by increasing the optical power.

In order to investigate the dielectric properties of the DAST crystal under different power of 532 nm laser irradiation, the complex refractive index $N_f(\omega)$ can be calculated based on THz reference signal $E_{sam}(\omega)$ and transmitted THz signal $E_{ref}(\omega)$ as follows:[28]

$$A e^{i\varphi} = \frac{E_{sam}(\omega)}{E_{ref}(\omega)}, \tag{1}$$

$$n(\omega) = 1 + \frac{\varphi c}{\omega d}, \tag{2}$$

$$\kappa(\omega) = -\frac{c}{d\omega} \ln\left(\frac{(n(\omega)+1)^2}{4n(\omega)} A\right), \tag{3}$$

$$N_{\rm f}(\omega) = n(\omega) + {\rm i}k(\omega), \tag{4}$$

where the amplitude transmittance $A = \sqrt{T}$ ($T$ is the transmitted THz intensity shown in Fig. 6(b)), $\varphi$ is the phase shift of the transmitted THz wave, $d$ is the sample thickness, $c$ is the light speed, $\omega$ is the frequency, and $n(\omega)$ and $k(\omega)$ are the refractive index and extinction coefficient, respectively. We calculated the refractive index and extinction coefficient by the above formulas, as shown in Figs. 8(a) and 8(b). It was showed that the refractive index of the DAST crystal decreased as the power of 532 nm laser increased, whereas the extinction coefficient showed an inverse tendency. When the power of 532 nm laser increased from 0 mW to 40 mW, the slight change was observed in the refractive index and extinction coefficient of the DAST crystal. With the power of 532 nm laser continually increasing, the decrease of refractive index and the increase of extinction coefficient were obviously observed.

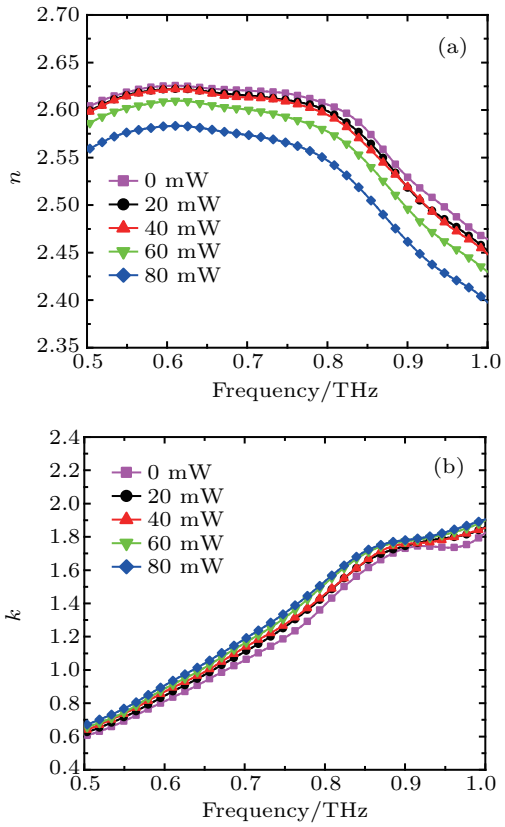



**Fig. 8.** (a) The refractive index and (b) extinction coefficient of DAST crystal excited by 532 nm laser at different power.

Figure 9 shows the variation of refractive index $\Delta n$ with the 532 nm laser power at 0.50 THz, 0.68 THz, and 0.85 THz. The variation of the refractive index of the DAST crystal caused by optical excitation was proportional to the square of the pump power. The applied optical field could make a contribution to the establishment of an internal electric field in the DAST crystal. The orientation of stilbazolium molecules (cation) and tosylate molecules (anion) in the DAST crystal would be rearranged in the internal electric field, which could result in the change of the third-order nonlinear polarizability in the DAST crystal. Thus, photorefractive phenomenon occurred because the average polarizability per molecule has been changed caused by the rearrangement of the molecular orientation.

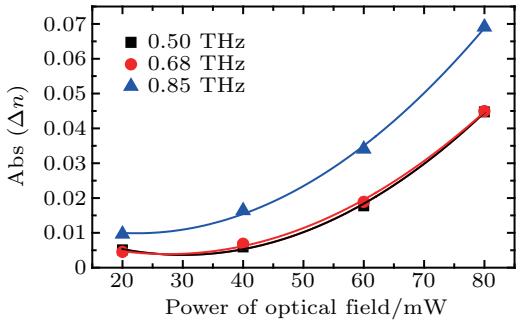



**Fig. 9.** The variation of refractive index $\Delta n$ under different 532 nm laser power at 0.50 THz, 0.68 THz, and 0.85 THz.

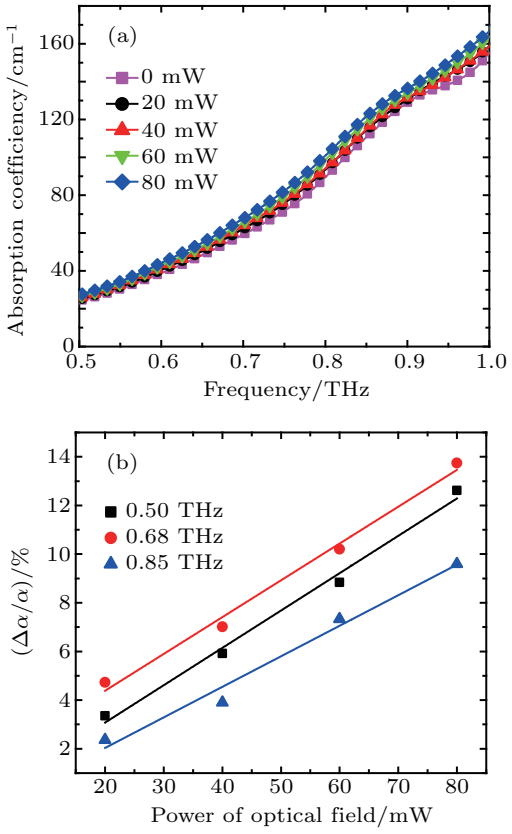



**Fig. 10.** (a) The absorption coefficient of DAST crystal under different 532 nm laser power. (b) The variation rate of absorption coefficient of DAST crystal at 0.50 THz, 0.68 THz, and 0.85 THz under different 532 nm laser power.

Furthermore, we calculated the absorption coefficient of the DAST crystal with the equation $\alpha(\omega) = 2\omega\kappa(\omega)/c$.[29] Figure 10(a) shows the absorption coefficient of the DAST crystal under different 532 nm laser power. As can be seen from Fig. 10(a), the absorption coefficient of the DAST crystal increased with the frequency of the THz wave. Especially, there was an increase in the absorption coefficient of the DAST crystal under external laser irradiation. The higher power of

the 532 nm laser irradiation, the larger increase of the absorption coefficient. The variation rate of the absorption coefficient of the DAST crystal at 0.50 THz, 0.68 THz, and 0.85 THz under different 532 nm laser power is depicted in Fig. 10(b). The linear behaviors were observed in the absorption coefficient versus the power of 532 nm laser irradiation, fitting well with the model of free carrier absorption induced by optical field. A significant enhancement of 13.7% in the THz absorption coefficient occurred at 0.68 THz due to the optically induced free carrier absorption effect in the DAST crystal.

## 4. Conclusion

In summary, optical-induced dielectric tunability properties of DAST crystal in THz range were experimentally investigated and theoretically analyzed. The experimental results showed that the transmitted THz intensity decreased by 26% at 0.68 THz when the power of the optical field was up to 80 mW. Meanwhile, the variation of refractive index showed an approximate quadratic behavior with the exciting optical field, which was related to the internal space charge field of photorefractive phenomenon in the DAST crystal caused by the photogenerated carrier. A significant enhancement of 13.7% for the THz absorption coefficient occurred at 0.68 THz due to the optically induced free carrier absorption effect in the DAST crystal. It is expected that DAST crystal with dielectric tunability properties could be further applied in the fields of THz modulation, biosensing, and detection.

## Acknowledgment

The authors are grateful for the the support of the 46th Research Institute of China Electronic Technology Group Corporation.

## References

[1] Lindsay G A, Davis M C, Chafin A P, Fallis S, Hoffman R C, Pritchett T M, Andzelm J, Rawlett A M, Park D and Herman W N 2009 *Opt. Mater.* **32** 302
[2] Somma C, Folpini G, Gupta J, Reimann K, Woerner M and Elsaesser T 2015 *Opt. Lett.* **40** 3404
[3] Li Z Y, Yao J Q, Lü D, Xu D G, Wang J L and Bing P B 2011 *Chin. Phys. Lett.* **28** 064209
[4] Qin Z B, Wen Y Q, Shang Y L, Song Y L and Wan Y Z 2007 *Appl. Phys. A* **87** 277
[5] Wang X Y, Wang J and Yang J H 2009 *Chin. Phys. Lett.* **26** 107502
[6] Ye H Q, Li Z, Peng Y, Wang C C, Li T Y, Zheng Y X, Sapelkin A, Adamopoulos G, Hernández I, Wyatt P B and Gillin W P 2014 *Nat. Mater.* **13** 382
[7] Meier U, Bösch M, Bosshard C, Pan F and Günter P 1998 *J. Appl. Phys.* **83** 3486
[8] Jagannathan K, Kalainathan S and Gnanasekaran T 2007 *Mater. Lett.* **61** 4485
[9] Jagannathan K and Kalainathan S 2007 *Mater. Res. Bull.* **42** 1881
[10] Takahashi Y, Sugiyama K, Brahadeeswaran S, Onzuka S, Kamimura T, Yoshimura M, Mori Y, Yoshida K and Sasaki T 2007 *Jan. J. Appl. Phys.* **46** 318
[11] Schneider A, Biaggio I and Günter P 2003 *Opt. Commun.* **224** 337
[12] He Y X, Wang Y Y, Xu D G, Nie M T, Yan C, Tang L H, Shi J, Feng J C, Yan D X, Liu H X, Teng B, Feng H and Yao J Q 2018 *Appl. Phys. B* **124** 16
[13] Qi F, Fan S, Notake T, Nawata K, Matsukawa T, Takida Y and Minamide H 2014 *Opt. Lett.* **39** 1294
[14] Ruiz B, Jazbinsek M and Günter P 2008 *Cryst. Growth.* **8** 4173
[15] Jagannathan K, Kalainathan S, Gnanasekaran T, Vijayan N and Bhagavannarayana G 2007 *Cryst. Growth.* **7** 859
[16] Jazbinsek M, Mutter L and Günter P 2008 *IEEE. J. Sel. Top. Quant.* **14** 1298
[17] Vijay R J, Melikechi N, Kumar T R, Jesudurai J and Sagayaraj P 2010 *J. Cryst. Growth* **312** 420
[18] Brahadeeswaran S, Onduka S, Takagi M, Takahashi Y, Adachi H, Kamimura T, Yoshimura M, Mori Y, Yoshida K and Sasaki T 2006 *Cryst. Growth.* **6** 2463
[19] Follonier S, Fierz M, Biaggio I, Meier U, Bosshard C and Günter P 2002 *J. Opt. Soc. Am. B* **19** 1990
[20] Chen L, Wei Y M, Zang X F, Zhu Y M and Zhuang S L 2016 *Sci. Rep.* **6** 22027
[21] Chen L, Liao D G, Guo X G, Zhao J Y, Zhu Y M and Zhuang S L 2019 *Front. Inform. Technol. Electron. Eng.* **20** 591
[22] Teng B, Wang S H, Feng K, Cao L F, Zhong D G, You F, Jiang X J, Hao L and Sun Q 2014 *Cryst. Res. Technol.* **49** 943
[23] Manikandan M R, Ram S D G and Ravi G 2012 *Adv. Mater. Res.* **584** 42
[24] Bosshard C, Spreiter R, Degiorgi L and Günter P 2002 *Phys. Rev. B* **66** 205107
[25] Cunningham P D and Hayden L M 2010 *Opt. Express* **18** 23620
[26] Deibel C, Strobel T and Dyakonov V 2010 *Adv. Mater.* **22** 4097
[27] Scarongella M, Laktionov A, Rothlisberger U and Banerji N 2013 *J. Mater. Chem. C* **1** 2308
[28] Yan D X, Xu D G, Li J N, Wang Y Y, Liang F, Wang J, Yan C, Liu H X, Shi J, Tang L H, He Y X, Zhong K, Lin Z S, Zhang Y W, Cheng H J, Shi W, Yao J Q and Wu Y C 2018 *Opt. Mater.* **78** 484
[29] Luo C Y, Ji J, Yue J, Rao Y K, Yao G, Li D, Zeng Y, Li R K, Xiao L S, Liu X X, Yao J Q and Ling F 2016 *Opt. Mater.* **60** 383